NASA/TM-2001-211262

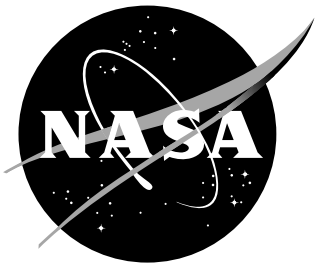

Computation of Flow Over a Drag Prediction Workshop Wing/Body Transport Configuration Using CFL3D

Christopher L. Rumsey and Robert T. Biedron
Langley Research Center, Hampton, Virginia

December 2001

The NASA STI Program Office ... in Profile

Since its founding, NASA has been dedicated to the advancement of aeronautics and space science. The NASA Scientific and Technical Information (STI) Program Office plays a key part in helping NASA maintain this important role.

The NASA STI Program Office is operated by Langley Research Center, the lead center for NASA's scientific and technical information. The NASA STI Program Office provides access to the NASA STI Database, the largest collection of aeronautical and space science STI in the world. The Program Office is also NASA's institutional mechanism for disseminating the results of its research and development activities. These results are published by NASA in the NASA STI Report Series, which includes the following report types:

- TECHNICAL PUBLICATION. Reports of completed research or a major significant phase of research that present the results of NASA programs and include extensive data or theoretical analysis. Includes compilations of significant scientific and technical data and information deemed to be of continuing reference value. NASA counterpart of peer-reviewed formal professional papers, but having less stringent limitations on manuscript length and extent of graphic presentations.

- TECHNICAL MEMORANDUM. Scientific and technical findings that are preliminary or of specialized interest, e.g., quick release reports, working papers, and bibliographies that contain minimal annotation. Does not contain extensive analysis.

- CONTRACTOR REPORT. Scientific and technical findings by NASA-sponsored contractors and grantees.

- CONFERENCE PUBLICATION. Collected papers from scientific and technical conferences, symposia, seminars, or other meetings sponsored or co-sponsored by NASA.

- SPECIAL PUBLICATION. Scientific, technical, or historical information from NASA programs, projects, and missions, often concerned with subjects having substantial public interest.

- TECHNICAL TRANSLATION. English-language translations of foreign scientific and technical material pertinent to NASA's mission.

Specialized services that complement the STI Program Office's diverse offerings include creating custom thesauri, building customized databases, organizing and publishing research results ... even providing videos.

For more information about the NASA STI Program Office, see the following:

- Access the NASA STI Program Home Page at ***http://www.sti.nasa.gov***

- E-mail your question via the Internet to help@sti.nasa.gov

- Fax your question to the NASA STI Help Desk at (301) 621-0134

- Phone the NASA STI Help Desk at (301) 621-0390

- Write to:
  NASA STI Help Desk
  NASA Center for AeroSpace Information
  7121 Standard Drive
  Hanover, MD 21076-1320

NASA/TM-2001-211262

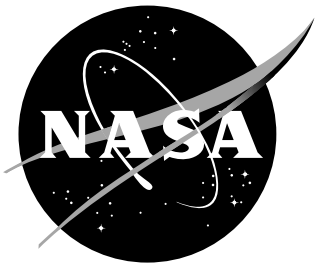

Computation of Flow Over a Drag Prediction Workshop Wing/Body Transport Configuration Using CFL3D

Christopher L. Rumsey and Robert T. Biedron
Langley Research Center, Hampton, Virginia

National Aeronautics and
Space Administration

Langley Research Center
Hampton, Virginia 23681-2199

December 2001

Available from:

NASA Center for AeroSpace Information (CASI)
7121 Standard Drive
Hanover, MD 21076-1320
(301) 621-0390

National Technical Information Service (NTIS)
5285 Port Royal Road
Springfield, VA 22161-2171
(703) 605-6000

Computation of Flow Over a Drag Prediction Workshop Wing/Body Transport Configuration Using CFL3D

Christopher L. Rumsey and Robert T. Biedron
NASA-Langley Research Center
Hampton, VA 23681-2199

Abstract

A Drag Prediction Workshop was held in conjunction with the 19th AIAA Applied Aerodynamics Conference in June 2001. The purpose of the workshop was to assess the prediction of drag by computational methods for a wing/body configuration (DLR-F4) representative of subsonic transport aircraft. This report details computed results submitted to this workshop using the Reynolds-averaged Navier-Stokes code CFL3D. Two supplied grids were used: a point-matched 1-to-1 multi-block grid, and an overset multi-block grid. The 1-to-1 grid, generally of much poorer quality and with less streamwise resolution than the overset grid, is found to be too coarse to adequately resolve the surface pressures. However, the global forces and moments are nonetheless similar to those computed using the overset grid. The effect of three different turbulence models is assessed using the 1-to-1 grid. Surface pressures are very similar overall, and the drag variation due to turbulence model is 18 drag counts. Most of this drag variation is in the friction component, and is attributed in part to insufficient grid resolution of the 1-to-1 grid. The misnomer of "fully turbulent" computations is discussed; comparisons are made using different transition locations and their effects on the global forces and moments are quantified. Finally, the effect of two different versions of a widely used one-equation turbulence model is explored.

1 Introduction

Drag prediction for aircraft by Reynolds-averaged Navier-Stokes (RANS) computational fluid dynamics (CFD) codes is currently an inexact science. Even for benign cruise-type conditions, the accuracy or confidence-level of CFD drag numbers is insufficient in comparison to the levels desired by the aircraft design industry. There are two issues of concern: (1) a given CFD code often does not agree with experiment in terms of the absolute drag numbers, and (2) different CFD codes and/or different turbulence models exhibit an excessively large variability. Usually, CFD can only be relied upon to perform trade studies, in which increments, rather than absolute levels, are predicted.

The first problem of disagreement with experimental absolute levels can be due to several causes. Probably the most significant is that CFD rarely models the same problem as experiment, especially for complex configurations. Neglecting wind tunnel walls, stings, small components, gaps between components, aeroelastic deformations, etc. can all have a significant impact on the results. Another important cause is underresolution; the CFD grid may not be fine enough to adequately resolve important features of the flow field. A further consideration is modeling errors, due to incorrect or incomplete model or theory. The most significant source of modeling error in most CFD computations is the turbulence model, including transition effects. Finally, the use of RANS itself can come under question for flows with massive separation, or other inherent unsteadiness.

The second problem of large variability among different CFD codes can arise from many sources. One is the differences in the basic numerical methods employed. Different schemes usually possess inherently different accuracy levels. This source of variability is also related to the problem of underresolution: differences in numerical implementations manifest themselves more noticeably on underresolved grids. Another source is different turbulence model variations (minor tweaks to constants, etc.), as well as different implementations of ostensibly the *same* turbulence model. Finally, coding differences such as limiters, explicit dissipation parameters, handling of inter-zone transfer information, boundary condition implementation, etc. can introduce variability.

For the Drag Prediction Workshop, although comparative agreement with absolute drag levels from three wind tunnel experiments was of interest, the primary purpose was to assess the variability among current state-of-the-art CFD codes. The overall variability is not covered here in detail; it is published elsewhere [1]. The current paper addresses only results from a single code. It includes some parametric studies on the effects of grid, turbulence model, and transition.

2 Numerical Method

The CFD code used is CFL3D [2], a widely-used structured-grid upwind finite-volume method. It neglects viscous cross-derivative terms, which results in the thin-layer Navier-Stokes equations in specified coordinate directions. Third-order upwind-biased spatial differencing on the convective and pressure terms, and second-order differencing on the viscous terms are used; it is globally second-order spatially accurate. The CFL3D code can solve flow over multiple-zone grids that are connected in a one-to-one, patched, or overset manner, and can employ grid sequencing, multi-grid, and local time stepping when accelerating convergence to steady state. Upwind-biased spatial differencing is used for the inviscid terms, and flux limiting is used to obtain smooth solutions in the vicinity of shock waves, when present. Viscous terms are centrally differenced.

The flux difference-splitting (FDS) method of Roe is employed to obtain fluxes at the cell faces. The CFL3D code is advanced in time with an implicit three-factor approximate factorization method. The implicit derivatives are written as spatially first-order accurate, which results in block-tridiagonal inversions for each sweep. However, for solutions that use FDS the block-tridiagonal inversions are further simplified with a diagonal

algorithm. Turbulence equations are solved uncoupled from the mean equations.

Three different turbulence models are employed. The first is the one-equation Spalart-Allmaras (SA) model [3], The second is a two-equation k-ω shear stress transport model due to Menter (SST) [4], and the third is an explicit algebraic stress model based on the two-equation k-ω formulation (EASM) [5]. The first two models are linear eddy viscosity models that employ the Boussinesq eddy viscosity assumption, while the third is a nonlinear eddy viscosity model.

For each of these turbulence models, there are several versions with minor variations in use today. However, in this report we only explore a little-known variation of the SA model in order to assess the type of differences that might be expected. CFL3D employs the version of SA referred to as SA-Ia. This is the version of the model that is given in Spalart and Allmaras [3], and will be referred to simply as "SA" from now on. There is also a version of SA in wide use that is unpublished: it employs an additional term f_{v3} that multiplies part of the source term. From now on, this unpublished version will be referred to as SA+fv3. The differences can be summarized as follows (refer to Spalart and Allmaras [3] for the form of the transport equation):

Version SA:

$$\hat{S} = \Omega + \frac{\hat{\nu} f_{v2}}{\kappa^2 d^2} \tag{1}$$

$$f_{v2} = 1 - \frac{\chi}{1 + \chi f_{v1}} \tag{2}$$

Version SA+fv3:

$$\hat{S} = f_{v3}\Omega + \frac{\hat{\nu} f_{v2}}{\kappa^2 d^2} \tag{3}$$

$$f_{v2} = \frac{1}{(1 + \chi/C_{v2})^3} \tag{4}$$

$$f_{v3} = \frac{(1 + \chi f_{v1})(1 - f_{v2})}{\chi} \tag{5}$$

The unpublished SA+fv3 model tends to delay boundary-layer transition relative to SA at moderately low Reynolds numbers (e.g., 1 to 10 million), even when the model is turned on everywhere ("fully turbulent"). At higher Reynolds numbers, the differences between the two versions are less significant.

3 Results

The experimental results for the DLR-F4 is detailed in Redeker [6]. Fig. 1 shows the wing-body configuration. Although the Drag Prediction Workshop specified several mandatory and optional cases [7], only the mandatory cases were computed here, and some of the parametric studies did not include all mandatory cases. Table 1 lists all of the cases performed in the present study, along with the resulting integrated forces and moments. All were at a Mach number of $M = 0.75$ and a Reynolds number (based on reference

chord of 141.2 mm) of 3 million. Note that one of the required cases was a solution at a $C_L = 0.5$. On the supplied 1-to-1 grid, an angle of attack of $\alpha = -0.345°$ achieved this.

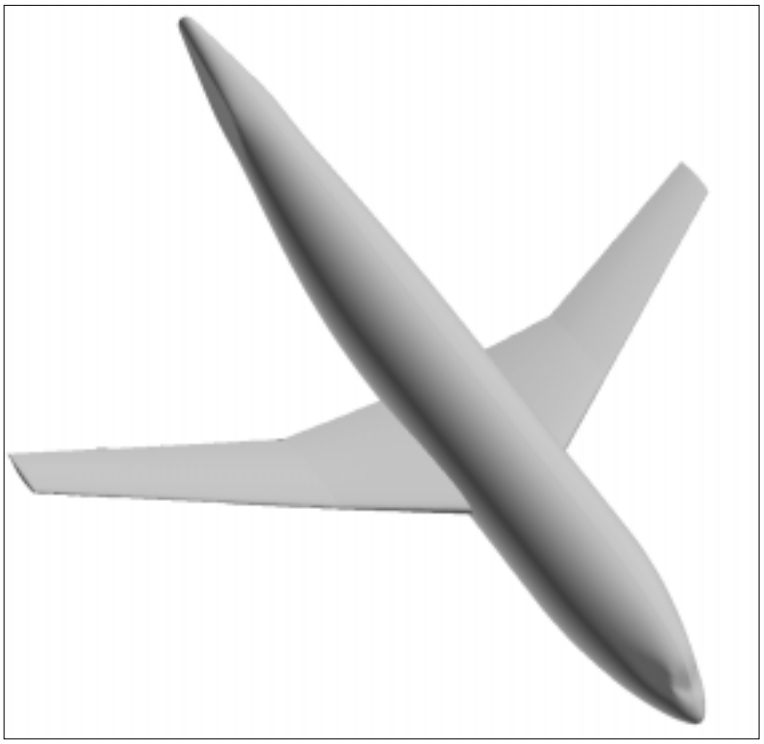

Figure 1: DLR-F4 wing-body configuration.

3.1 Effect of Grid

A grid convergence study was performed for the 1-to-1 grid using coarser levels (every other point in each direction) from the supplied grid. The supplied grid contains approximately 3.2 million points. The supplied grid models only half of the configuration; symmetry boundary conditions are used to simulate the full configuration as shown in Fig. 1. Creating a medium level grid using every other point yields approximately 400,000 points, and a coarse level grid yields approximately 50,000 points. The three grid levels were run at the same $C_L = 0.5$ condition using SA. For the three grid levels (fine, medium, and coarse), this corresponds to angles of attack of -0.345, -0.145, and 0.107, respectively.

Results are shown in Fig. 2. C_D is plotted against $N^{-2/3}$, where N is the total number of grid cells. For a second-order spatially-accurate scheme, this plot should yield a linear variation in C_D. Clearly, this is not the case. The coarse level grid is certainly too coarse to be in the asymptotic region of the grid convergence plot. If we assume that the medium and fine level grids are both in the asymptotic region, and extrapolate to an infinite-density result, then the extrapolated drag is 0.0284. This level is approximately 30 drag counts (0.0030) lower than the result (0.03145) on the supplied fine grid! However, based on experience, 400,000 points is insufficient to adequately resolve a 3-D wing-body

Table 1: Summary of cases run

Grid	α, deg	Turb model	Transition	C_L	C_M	C_D
1-to-1	-3.0	SA	"fully turbulent"	0.176	-0.1713	0.02270
1-to-1	-2.0	SA	"fully turbulent"	0.299	-0.1708	0.02481
1-to-1	-1.0	SA	"fully turbulent"	0.420	-0.1685	0.02830
1-to-1	-0.345	SA	"fully turbulent"	0.500	-0.1656	0.03145
1-to-1, medium	-0.145	SA	"fully turbulent"	0.500	-0.1561	0.04057
1-to-1, coarse	0.107	SA	"fully turbulent"	0.500	-0.1468	0.06485
1-to-1	0.0	SA	"fully turbulent"	0.542	-0.1633	0.03346
1-to-1	1.0	SA	"fully turbulent"	0.663	-0.1550	0.04168
1-to-1	2.0	SA	"fully turbulent"	0.760	-0.1385	0.05417
1-to-1	-3.0	SST	"fully turbulent"	0.177	-0.1710	0.02095
1-to-1	-2.0	SST	"fully turbulent"	0.300	-0.1706	0.02303
1-to-1	-1.0	SST	"fully turbulent"	0.421	-0.1682	0.02651
1-to-1	-0.345	SST	"fully turbulent"	0.500	-0.1650	0.02964
1-to-1	0.0	SST	"fully turbulent"	0.542	-0.1629	0.03164
1-to-1	1.0	SST	"fully turbulent"	0.666	-0.1559	0.03997
1-to-1	2.0	SST	"fully turbulent"	0.759	-0.1374	0.05245
1-to-1	-3.0	EASM	"fully turbulent"	0.179	-0.1711	0.02088
1-to-1	-2.0	EASM	"fully turbulent"	0.301	-0.1706	0.02295
1-to-1	-1.0	EASM	"fully turbulent"	0.422	-0.1680	0.02642
1-to-1	-0.345	EASM	"fully turbulent"	0.500	-0.1644	0.02953
1-to-1	0.0	EASM	"fully turbulent"	0.542	-0.1619	0.03152
1-to-1	1.0	EASM	"fully turbulent"	0.668	-0.1559	0.03992
1-to-1	2.0	EASM	"fully turbulent"	0.771	-0.1422	0.05280
1-to-1	0.0	SA+fv3	"fully turbulent"	0.552	-0.1687	0.03332
1-to-1	0.0	SA	set same as EASM	0.543	-0.1640	0.03342
overset	-1.0	SA	"fully turbulent"	0.418	-0.1639	0.02792
overset	0.0	SA	"fully turbulent"	0.541	-0.1570	0.03266

configuration, so it is doubtful that the medium level grid is fine enough to be in the asymptotic region. Thus, it is impossible to know how well-converged the supplied fine-level grid is without additional runs on even finer grids, which were not available for the workshop.

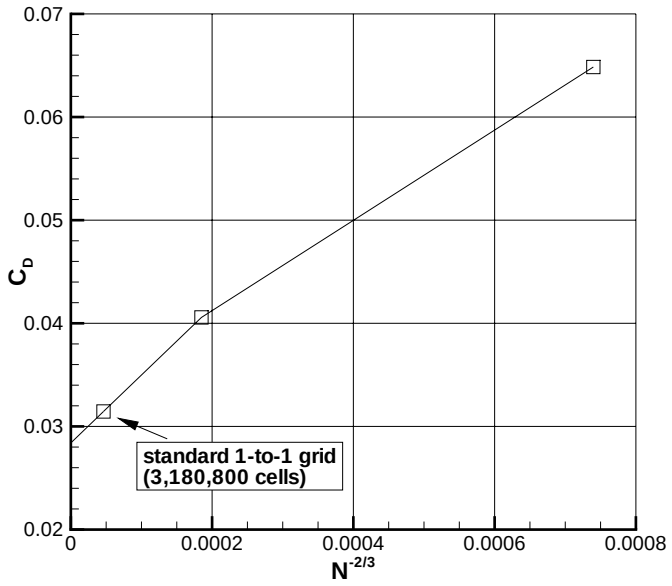

Figure 2: Grid convergence for 1-to-1 grid at $C_L = 0.5$, SA.

Although most of the results in this study used the supplied 1-to-1 grid, the supplied overset grid was also employed for a few cases. A spanwise cut of the two grids near a span location of $y = 230$ mm is shown in Fig. 3. Several significant differences are evident from this comparison. The 1-to-1 grid has fewer streamwise points (around the airfoil): 153 as opposed to 257 for the overset grid. Furthermore, from the grid quality standpoint, the 1-to-1 grid has grid lines that do not come in perpendicular to the wing surface, the grid spacing is quite coarse at the leading edge, and there are several areas where the grid spacing changes discontinuously when passing from one zone to the next. Although not shown, the 1-to-1 grid has a far field extent of approximately 50 mean aerodynamic chords, whereas the overset grid has an extent approximately 3 times as far. The total number of grid points is similar: 3.2 million for the 1-to-1 and 3.7 million for the overset.

The effect of grid topology (overset vs. 1-to-1) on surface pressure coefficient is shown in Fig. 4 at seven span stations. Computed results were made at $\alpha = 0°$. Although it is not a direct comparison, experimental results *at a fixed* C_L of 0.5 are shown for reference. The computed C_L levels are 0.541 and 0.542 for the overset grid and 1-to-1 grid, respectively. It is evident from this figure that the 1-to-1 grid yields a more smeared-out shock, particularly at the outboard stations. Also, the same pressure peak level is not attained near the leading edge as with the overset grid. However, results near the wing trailing edge and on the lower surface are very similar.

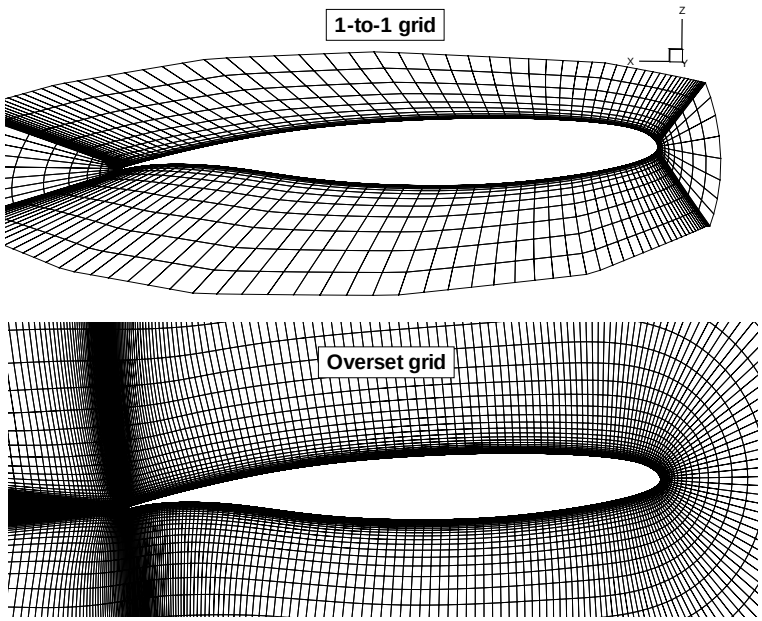

Figure 3: Comparison of supplied grids near $y = 230$ mm ($2y/B = 0.391$).

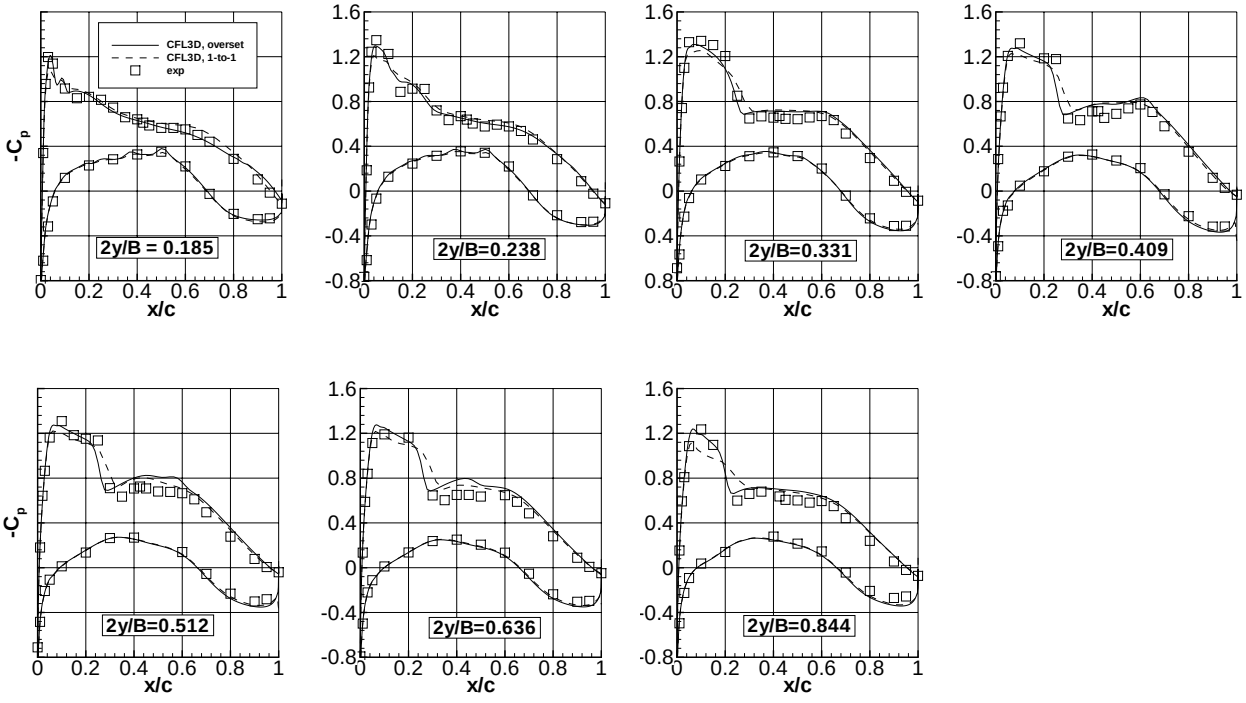

Figure 4: Effect of grid topology on surface pressure coefficient, $\alpha = 0°$, SA.

Integrated forces and moments do not show much difference between results using the two grids. Lift, moment, and drag levels are shown in Figs. 5, 6, and 7, respectively. The experimental data from 3 different facilities are plotted together, giving an indication of the uncertainty associated with experiments. At $\alpha = 0°$, lift using the two grids differs by 0.2%, moment by 4.0%, and drag by 2.4%. The total drag values are broken into their component pressure drag (C_{Dp}) and viscous drag (C_{Dv}) values in Fig. 8.

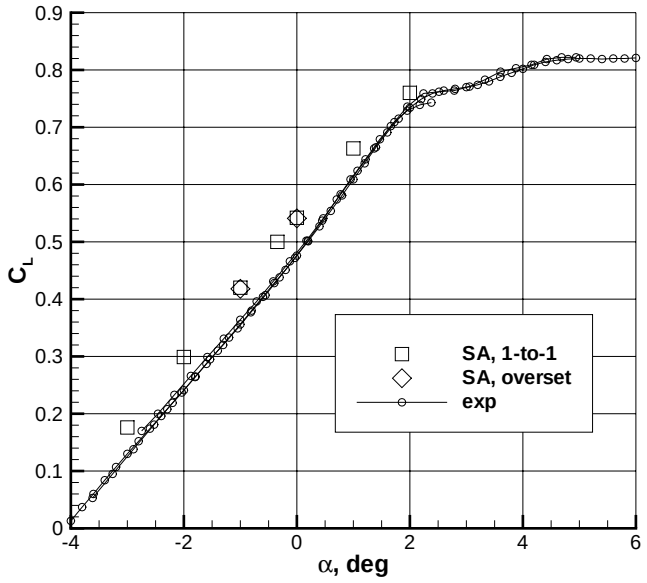

Figure 5: Effect of grid topology on lift coefficient, SA.

3.2 Effect of Turbulence Model

The use of the three different turbulence models on the 1-to-1 grid had very little overall effect on results at any of the angles of attack tested. Surface pressure coefficients were surprisingly similar. For example, surface pressure coefficient is shown in Fig. 9 for an angle of attack of $\alpha = 2°$ (this angle of attack exhibits the largest differences between the models). Results are almost indistinguishable from each other; however, near the wing tip, the SST predicts the furthest forward shock location and the EASM the furthest aft.

If one looks in detail at surface streamlines for this case, very small differences can also be seen in the flowfield behavior between the shock and the wing trailing edge. Results are shown for SA, SST, and EASM in Figs. 10, 11, and 12, respectively. In all cases over much of the wing, the flow separates immediately behind the shock, then reattaches, then separates again near the trailing edge. The SA model exhibits the largest region of trailing edge separation, and EASM the smallest. EASM also predicts the smallest extent of separation behind the shock.

The turbulence model effects on integrated forces and moments are shown in Figs. 13,

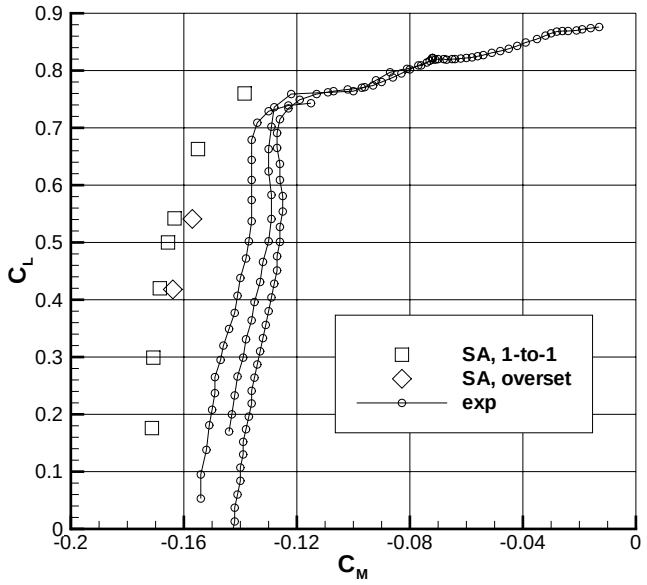

Figure 6: Effect of grid topology on moment coefficient, SA.

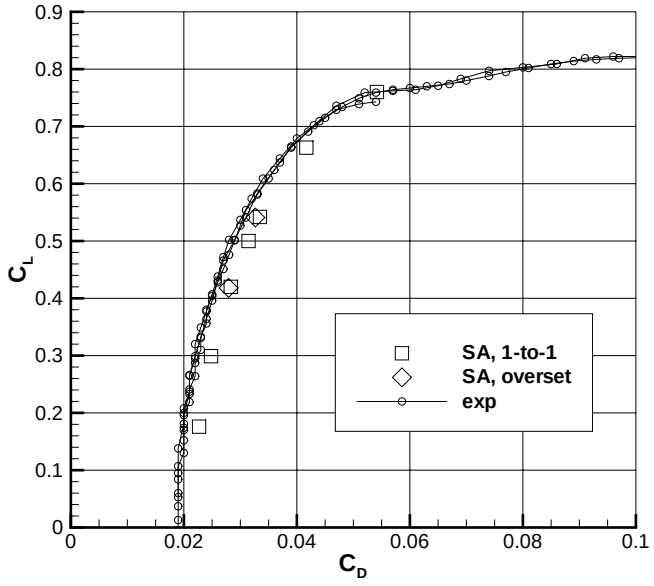

Figure 7: Effect of grid topology on drag coefficient, SA.

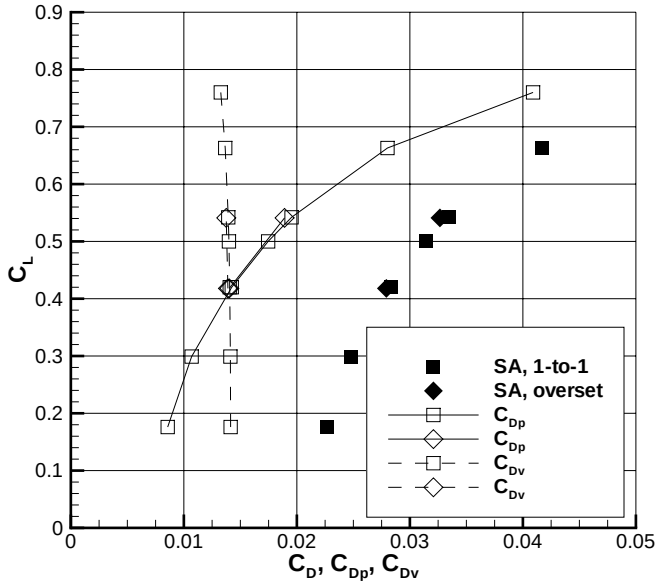

Figure 8: Effect of grid topology on pressure and viscous drag coefficient components, SA.

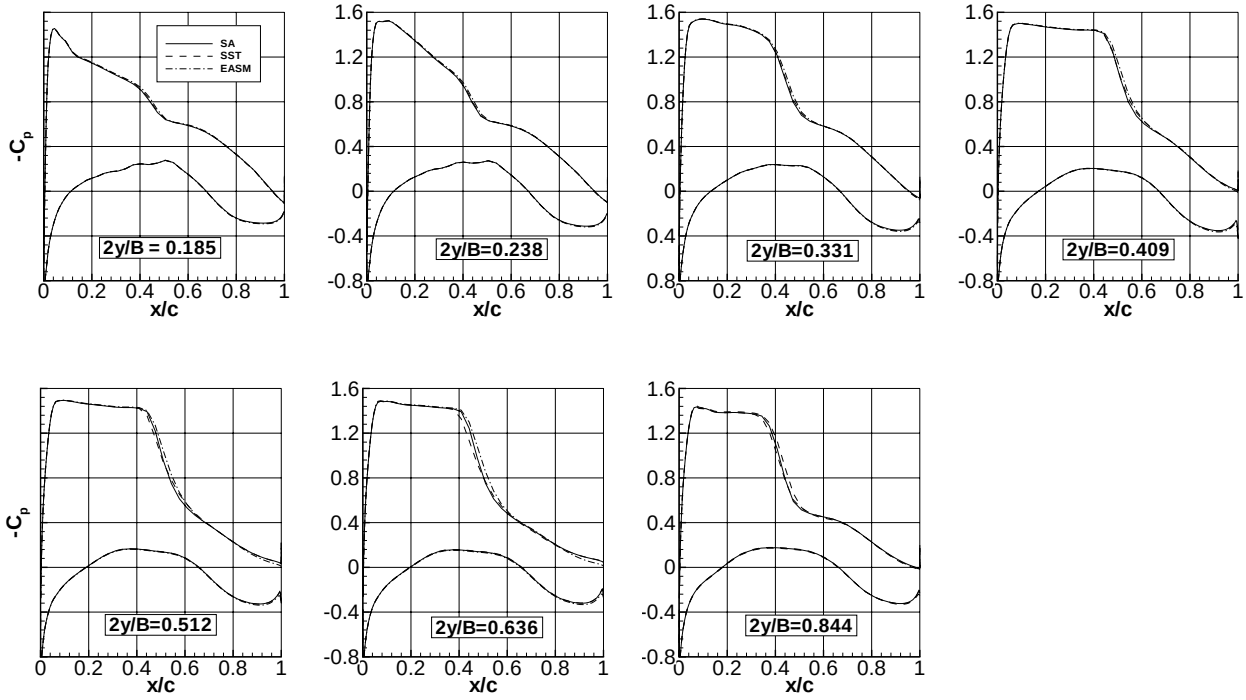

Figure 9: Effect of turbulence model on surface pressure coefficient, $\alpha = 2°$, 1-to-1 grid.

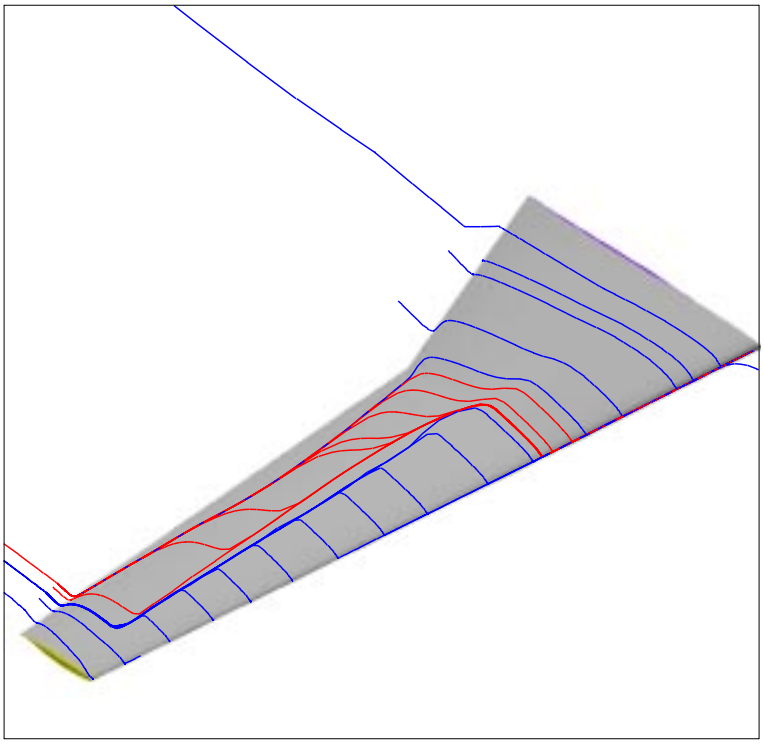

Figure 10: Wing upper surface streamlines at $\alpha = 2°$, SA, 1-to-1 grid.

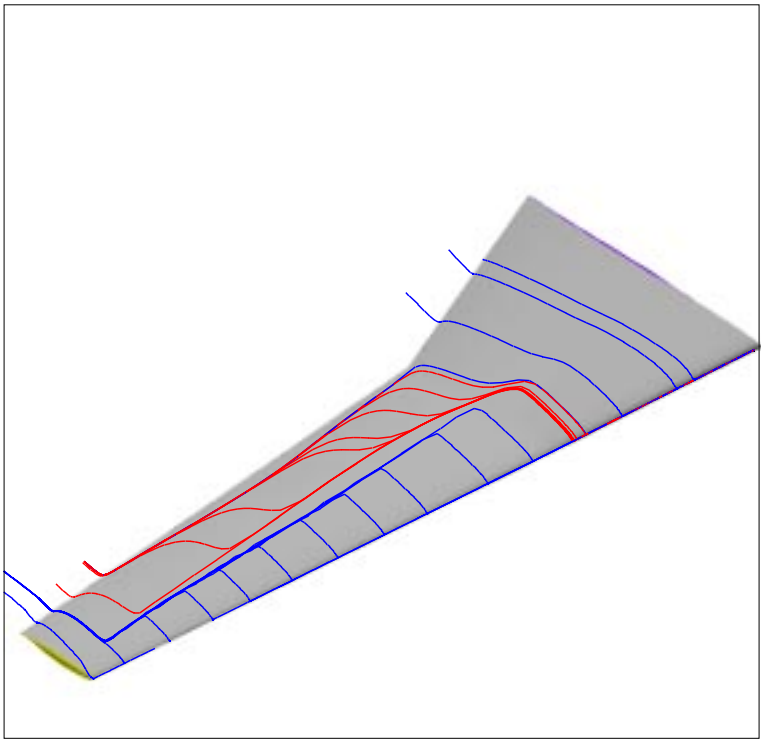

Figure 11: Wing upper surface streamlines at $\alpha = 2°$, SST, 1-to-1 grid.

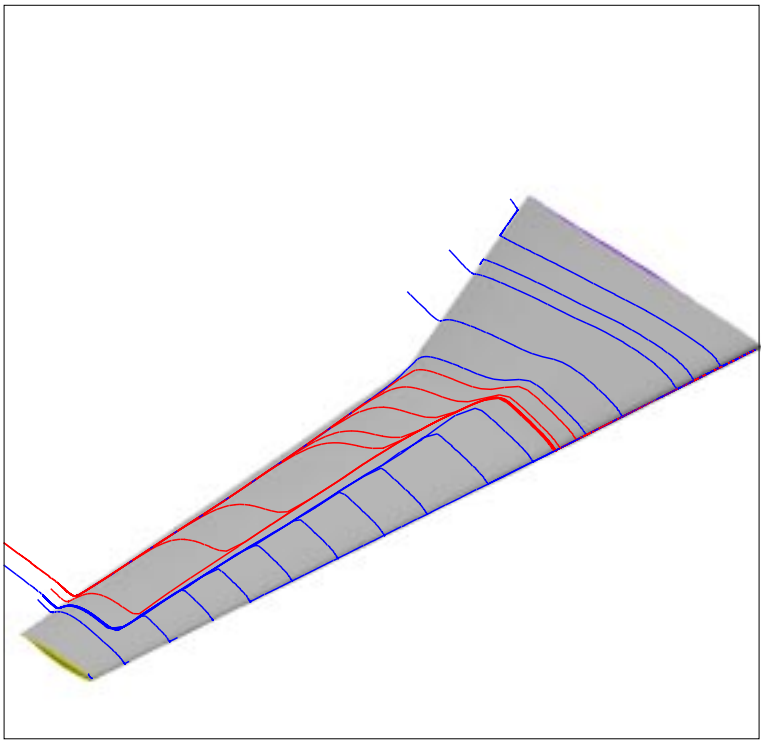

Figure 12: Wing upper surface streamlines at $\alpha = 2°$, EASM, 1-to-1 grid.

14, and 15. Very little effects are seen, in general, except that the drag for SST and EASM is consistently lower than SA across the angle of attack range. By looking in detail at the component drag forces in Fig. 16, it is seen that the pressure drag component is roughly the same for all three models, but the viscous drag component is lower for SST and EASM than SA by about 18 drag counts. These drag count differences are distributed approximately equally over the wing-body according to surface area: approximately 3 drag counts on the wing upper surface, 3 on the wing lower surface, and 12 on the body.

These differences can be better understood by looking at how the three models behave with grid refinement on a simpler problem. For a zero-pressure-gradient flat plate at a Reynolds number of 6 million per unit length, the skin friction coefficient at a location 75% down the length of the plate is plotted as a function of the inverse of the number of total grid points in Fig. 17. The finest grid level used for this problem is a 129×193, and each successively coarser grid is created by removing every other point from the finer grid. Even the coarsest grid has a minimum spacing at the wall so that its $y+$ value is less than 1. As the grid is refined, the results for the three models approach each other, to within 2.5% on the finest grid. (Note that results for the three models are not expected to be the same, even on a grid of infinite density, because of model calibration differences.) On coarser grids, SA yields *higher* skin friction (it approaches its resolved answer from above) whereas the SST and EASM yield *lower* skin frictions (they approach their resolved answers from below). In this simple 2-D example, doubling the grid in each coordinate direction has the effect of reducing the maximum difference between the skin friction levels by a factor of roughly 4.

Thus, if the behavior of this simple case holds for more complex 3-D configurations, then on an underresolved grid, one might expect the drag due to skin friction for SA to be significantly higher than that due to SST or EASM. Assuming second-order spatial accuracy and extrapolating the results from this example to the DLR-F4 case, the drag difference due to turbulence model would be expected to be about 11 drag counts on a similar 1-to-1 grid with twice the *total* number of points (6,400,000 cells), and less than 5 drag counts on a twice finer grid in each coordinate direction (25,600,000 cells).

Quantitatively, the largest difference between any two turbulence models at $\alpha = 0°$ is 0% in lift, 0.9% in moment, and 6.2% in drag (18 drag counts). The 18 count difference in drag (see Fig. 16) is approximately constant across the angle of attack range. In terms of percent difference, 18 drag counts corresponds to 8.7% at $\alpha = -3°$ and 3.3% at $\alpha = 2°$.

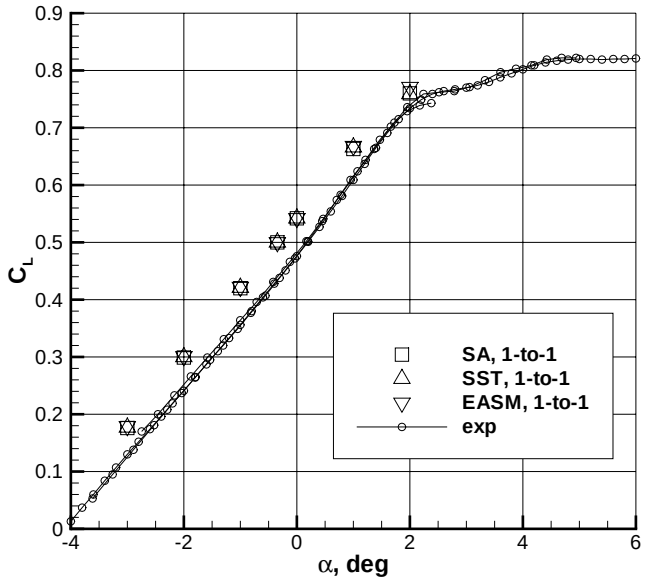

Figure 13: Effect of turbulence model on lift coefficient, 1-to-1 grid.

3.3 The Misnomer of "Fully Turbulent" Computations

Many CFD practitioners run "fully turbulent" computations with the expectation that the computed flow will indeed be fully turbulent everywhere. Unfortunately, this is not the case. "Fully turbulent" *does* indicate that the equations for the turbulent quantities are solved everywhere, but the source terms in the models (taken in combination with freestream levels of turbulence that are prescribed) are often not large enough to initiate turbulence until some distance downstream from the leading edges of solid bodies in the flow. Where the transition actually takes place is a strong function of the Reynolds number of the flow, the particular model being employed, and its freestream turbulent quantities.

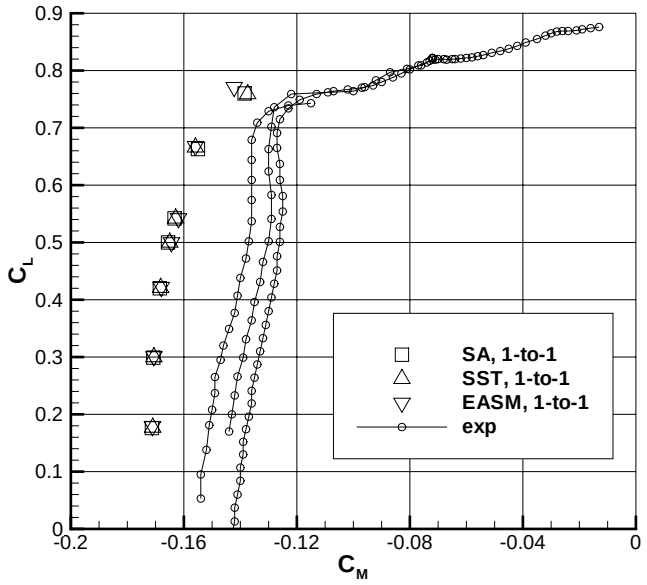

Figure 14: Effect of turbulence model on moment coefficient, 1-to-1 grid.

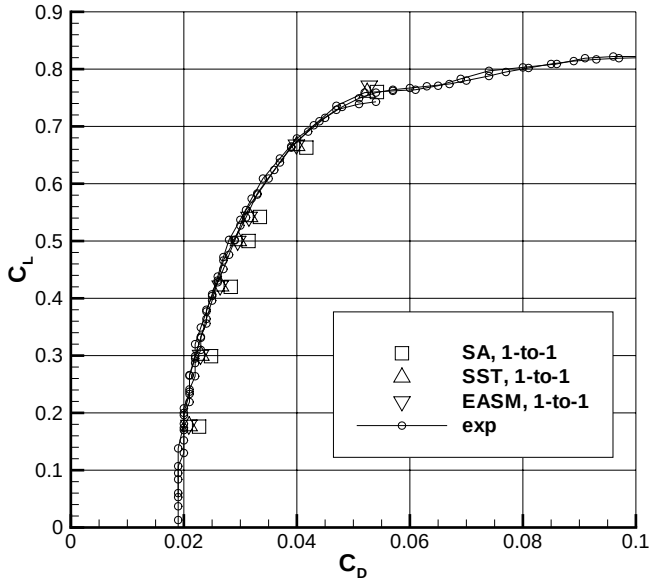

Figure 15: Effect of turbulence model on drag coefficient, 1-to-1 grid.

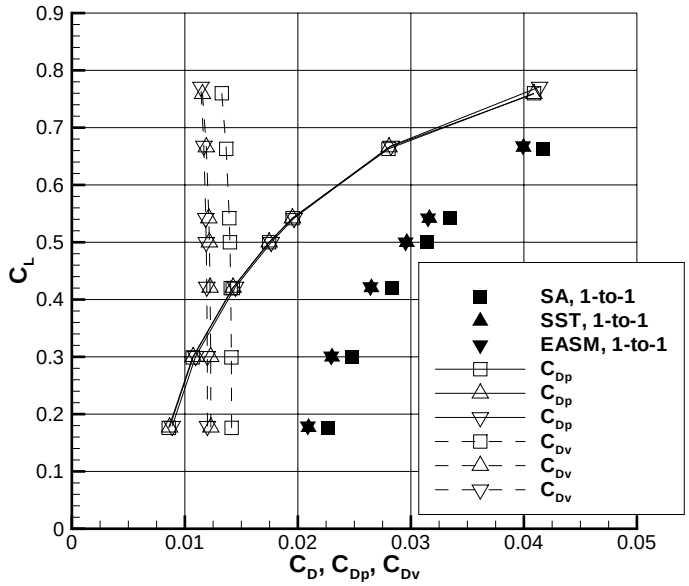

Figure 16: Effect of turbulence model on pressure and viscous drag coefficient components, 1-to-1 grid.

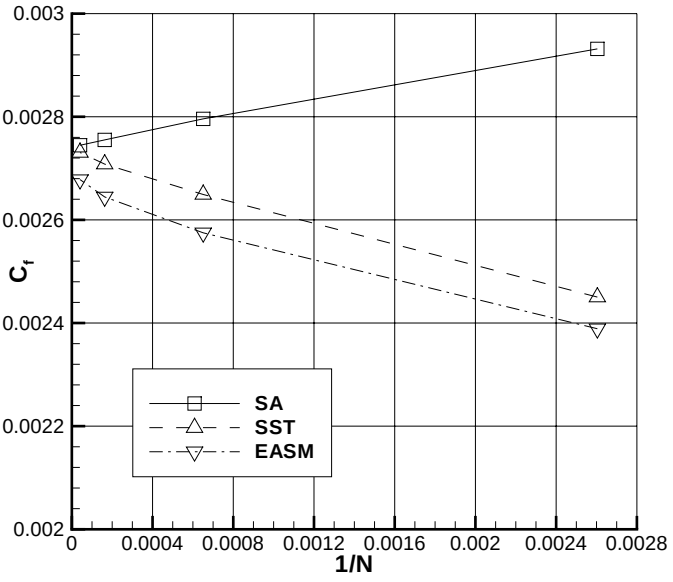

Figure 17: Skin friction coefficient at $x/L = 0.75$ for a zero-pressure-gradient flat plate, $\mathrm{Re}_L = 6$ million, for different turbulence models and different grid sizes.

It is good engineering practice to always check a CFD run after-the-fact to determine where the turbulent flow actually transitioned. One way to do this is to look for $\mu_{t,\max}$, the maximum eddy viscosity level, along grid lines normal to the surface. When $\mu_{t,\max}$ exceeds 1, the flow can be considered to be fully turbulent. Fig. 18 shows the upper surface transition locations for the three turbulence models for the $\alpha = 1°$ case. Although the flow was specified to be "fully turbulent," in each case it transitioned some distance downstream from the leading edge at this Reynolds number of 3 million. In this plot the 3 locations cannot be distinguished from each other; they are all very near the leading edge, especially at the inboard stations. Fig. 19 shows a close-up near the leading edge. The SA model transitions the furthest forward, at approximately 1.4%c at span station $y = 400$ mm, and the EASM transitions furthest aft, near 5.7%c.

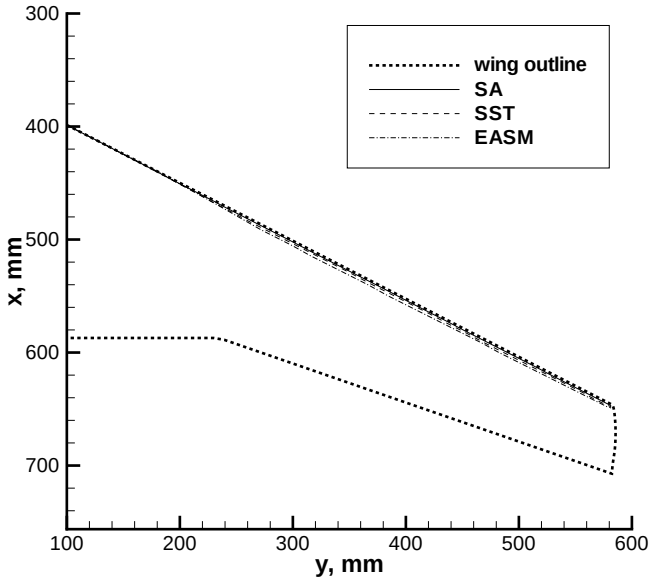

Figure 18: Upper surface transition locations at $\alpha = 0°$ for "fully turbulent" computations, 1-to-1 grid.

The effect of these various transition locations on drag coefficient was investigated by *forcing* the SA model to transition at roughly the same upper and lower surface locations as EASM. (This delay of transition is accomplished in CFL3D by setting the turbulence model source terms to zero in the region where laminar flow is desired.) Results are plotted in Fig. 20. This figure shows almost no difference in the computed drag values due to this small change in transition location. The difference at $\alpha = 0°$ is 0.2% in lift, 0.4% in moment, and 0.1% in drag.

3.4 Effect of SA Version

The effects of the different versions of SA are shown in Fig. 21 and 22. Although not shown, at $\alpha = 0°$ the SA+fv3 delays transition to typically 7 - 8%c over much of the

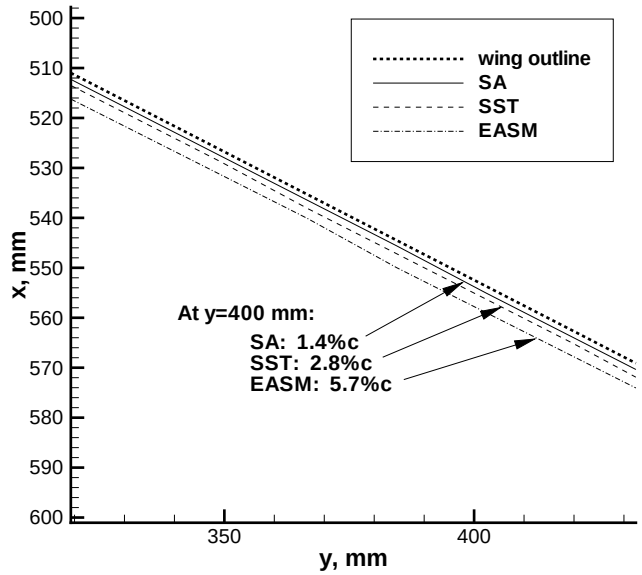

Figure 19: Detail of upper surface transition locations at $\alpha = 0°$ for "fully turbulent" computations, 1-to-1 grid.

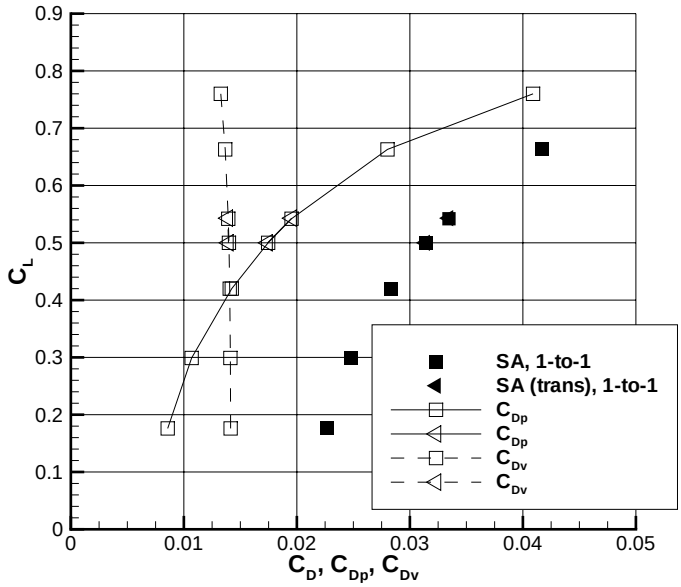

Figure 20: Effect of forcing SA to transition at the same location as EASM on pressure and viscous drag coefficient components, 1-to-1 grid.

span, compared to 1 - 2%c for SA. Overall, the effect is relatively small in the integrated quantities. The difference is 1.8% in lift, 3.3% in moment, and 0.4% in drag (the moment plot is not shown).

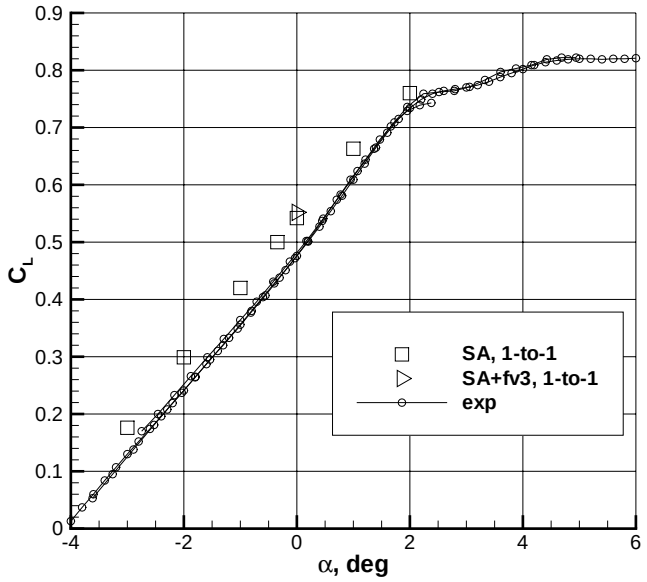

Figure 21: Effect of different versions of "fully turbulent" SA on lift coefficient, 1-to-1 grid.

4 Summary

As a part of a participation in the Drag Prediction Workshop using CFL3D, four effects were examined for the DLR-F4 wing-body configuration: effect of grid, effect of turbulence model, effect of transition location for "fully turbulent" computations, and effect of two different versions of the SA model. Most of these parametric studies employed the 1-to-1 multi-block grid supplied by the Drag Workshop committee (and subsets thereof), while a few cases used the supplied overset grid.

Unfortunately, the supplied 1-to-1 grid turned out to be not only too coarse to resolve surface pressures adequately, but it also was of overall very poor quality. Both of these factors make many of the conclusions from the current study only tentative, because it it preferable to have confidence in the grid-independence of solutions before drawing conclusions regarding turbulence model effects, transition effects, etc. In a more well-designed study, a family of grids (2 or 3 for each type, 1-to-1 and overset) would be employed, including at least one grid that is significantly finer than the current supplied grids.

In spite of differences between the supplied 1-to-1 grid and overset grid predicted surface pressures, global forces and moments were very similar. For example, at $\alpha = 0°$,

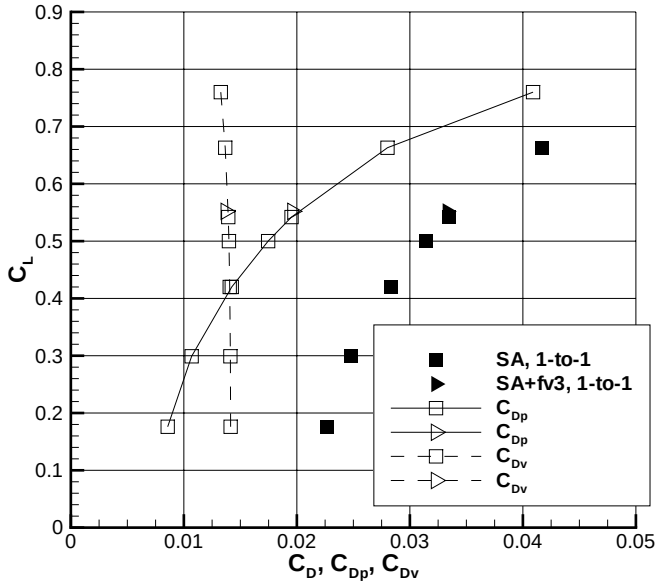

Figure 22: Effect of different versions of "fully turbulent" SA on pressure and viscous drag coefficient components, 1-to-1 grid.

the C_D yielded only an 8 count difference (0.0008), or 2.4%. This effect is shown in a summary plot in Fig. 23, along with the effect of the grid on the lift and moment.

Also shown in this figure are the other effects studied on the 1-to-1 grid. The three turbulence models gave overall very similar results, with the largest difference in the drag of approximately 18 counts (0.0018), or 6.2% at $\alpha = 0°$. This difference was primarily due to differences in the friction drag. On the basis of a systematic study of accuracy with grid refinement for a model problem, the difference is expected to decrease to less than 5 counts on a twice finer grid in each coordinate direction.

The phrase "fully turbulent" as applied to CFD computations is a misnomer. In spite of the fact that the turbulence equations are turned on everywhere, each model may or may not yield turbulent flow immediately at the leading edge, and each model's transition location is generally different from other models. For the current DLR-F4 case, the SA model transitions the furthest forward (generally between 1 - 2%c) and the EASM the furthest back (generally between 2 - 7%c), but the effect of varying the transition location the small amount between the "fully turbulent" location for SA to the "fully turbulent" location for EASM was very small. See Fig. 23 under the label "trans loc."

Two different versions of the SA model, known to be present in today's U.S. production codes, were described. The unpublished SA+fv3 version can delay transition significantly for low Reynolds number flows. The effect for the current case on the 1-to-1 grid is shown in Fig. 23, as "SA version." At $\alpha = 0°$, the difference in C_D is only 1.4 counts (0.00014), or 0.4%.

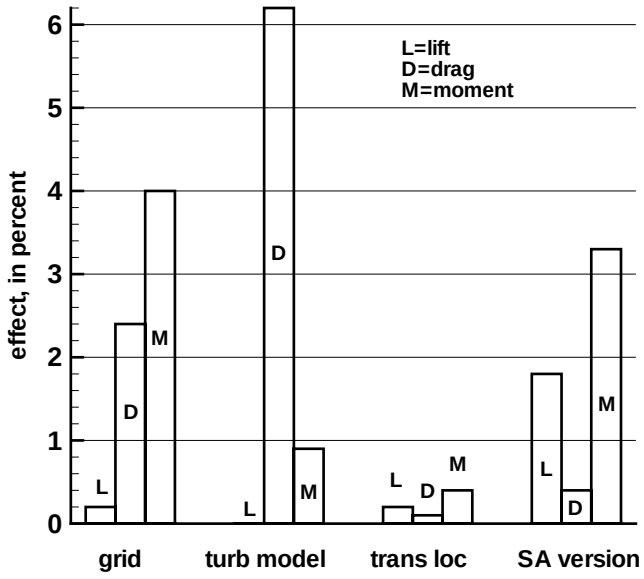

Figure 23: Summary of effects at $\alpha = 0°$ (1-to-1 grid is reference grid).

5 Conclusions and Recommendations

Some general conclusions to be made from the current study are as follows:

- Good grid quality and sufficient grid density are of first order importance, and the benefit of a grid study cannot be overstated. Many of the conclusions of the current parametric investigations are clouded by the fact that the 1-to-1 grid used was not sufficiently fine and possessed poor orthogonality and smoothness characteristics.
- The three turbulence models investigated showed some relatively minor differences, but overall they gave very similar predictions over the entire angle of attack range, even when separated flow was present.
- CFD transition location should always be checked. "Fully turbulent" computations usually exhibit a transition location downstream of the leading edge, especially at low Reynolds numbers (e.g., 1 - 10 million), and the location is usually different for different models.
- Better version control and consistency checks are needed for turbulence model coding. Currently, different versions of the Spalart-Allmaras model are being employed in different U.S. production codes under ostensibly the same name of "SA." These two versions can produce different transition locations for "fully turbulent" computations.

Some recommendations for future drag prediction workshops of this type are also given here:

- Give out a family of successively finer grids for a required grid study. Supplying official grids ensures consistency among participants. For a wing-body configuration, the finest grid supplied should have *at least* 7 million points.

- Include surface C_p predictions as a part of the required results. This is important because integrated quantities such as lift, drag, and moment can mask problems that may be helpful in subsequent evaluations.

- Require more fixed-α cases, and fewer fixed-C_L cases. Fixed-α cases are easier to run and are more meaningful for comparing code-to-code results (i.e., the *same* problem and boundary conditions are being simulated). Fixed-C_L cases are often used for comparing with experimental data, but they require significantly more computing resources and comparisons between codes can be more ambiguous.

- To ensure that transition location is not a cause of variability, either (1) ask participants to force transition at specified locations, or (2) include higher Reynolds number cases, where "fully turbulent" computations actually come out that way.

References

[1] Hemsch, M. J., "Statistical Analysis of CFD Solutions from the Drag Prediction Workshop," AIAA Paper 2002-0842, Reno, NV, January 2002.

[2] Krist S. L., Biedron R. T., and Rumsey C. L., "CFL3D User's Manual (Version 5.0)", NASA TM-1998-208444, June 1998.

[3] Spalart, P. R., and Allmaras, S. R., "A One-Equation Turbulence Model for Aerodynamic Flows," *La Recherche Aerospatiale*, No. 1, 1994, pp. 5–21.

[4] Menter, F. R., "Two-Equation Eddy-Viscosity Turbulence Models for Engineering Applications," *AIAA Journal*, Vol. 32, No. 8, 1994, pp. 1598–1605.

[5] Rumsey, C. L., and Gatski, T. B., "Recent Turbulence Model Advances Applied to Multielement Airfoil Computations," AIAA Paper 2000-4323, August 2000.

[6] Redeker, G., "DLR-F4 Wing Body Configuration," AGARD-AR-303, A Selection of Experimental Test Cases for the Validation of CFD Codes, Vol. 2, August 1994, pp. B4-1 – B4-21.

[7] Drag Prediction Website, 2001:
http://www.aiaa.org/tc/apa/dragpredworkshop/dpw.html

REPORT DOCUMENTATION PAGE

Form Approved
OMB No. 0704-0188

1. AGENCY USE ONLY *(Leave blank)*	2. REPORT DATE	3. REPORT TYPE AND DATES COVERED
	December 2001	Technical Memorandum

4. TITLE AND SUBTITLE
Computation of Flow Over a Drag Prediction Workshop Wing/Body Transport Configuration Using CFL3D

5. FUNDING NUMBERS
WU 706-31-11-80

6. AUTHOR(S)
Christopher L. Rumsey and Robert T. Biedron

7. PERFORMING ORGANIZATION NAME(S) AND ADDRESS(ES)
NASA Langley Research Center
Hampton, VA 23681-2199

8. PERFORMING ORGANIZATION REPORT NUMBER
L-18132

9. SPONSORING/MONITORING AGENCY NAME(S) AND ADDRESS(ES)
National Aeronautics and Space Administration
Washington, DC 20546-0001

10. SPONSORING/MONITORING AGENCY REPORT NUMBER
NASA/TM-2001-211262

11. SUPPLEMENTARY NOTES

12a. DISTRIBUTION/AVAILABILITY STATEMENT
Unclassified-Unlimited
Subject Category 02 Distribution: Nonstandard
Availability: NASA CASI (301) 621-0390

12b. DISTRIBUTION CODE

13. ABSTRACT *(Maximum 200 words)*
A Drag Prediction Workshop was held in conjunction with the 19th AIAA Applied Aerodynamics Conference in June 2001. The purpose of the workshop was to assess the prediction of drag by computational methods for a wing/body configuration (DLR-F4) representative of subsonic transport aircraft. This report details computed results submitted to this workshop using the Reynolds-averaged Navier-Stokes code CFL3D. Two supplied grids were used: a point-matched 1-to-1 multi-block grid, and an overset multi-block grid. The 1-to-1 grid, generally of much poorer quality and with less streamwise resolution than the overset grid, is found to be too coarse to adequately resolve the surface pressures. However, the global forces and moments are nonetheless similar to those computed using the overset grid. The effect of three different turbulence models is assessed using the 1-to-1 grid. Surface pressures are very similar overall, and the drag variation due to turbulence model is 18 drag counts. Most of this drag variation is in the friction component, and is attributed in part to insufficient grid resolution of the 1-to-1 grid. The misnomer of ``fully turbulent" computations is discussed; comparisons are made using different transition locations and their effects on the global forces and moments are quantified. Finally, the effect of two different versions of a widely used one-equation turbulence model is explored.

14. SUBJECT TERMS
Drag; Variability; Tubulence model

15. NUMBER OF PAGES
26

16. PRICE CODE

17. SECURITY CLASSIFICATION OF REPORT	18. SECURITY CLASSIFICATION OF THIS PAGE	19. SECURITY CLASSIFICATION OF ABSTRACT	20. LIMITATION OF ABSTRACT
Unclassified	Unclassified	Unclassified	UL